Res Chem Intermed (2015) 41:8907–8927
DOI 10.1007/s11164-015-1937-1

Mn(Salen)Cl complexes immobilized on SBA-15 functionalized with amine as an efficient, selective and recyclable catalyst for benzyl alcohol oxidation by TBHP: the effects of Mn loading and reaction conditions

Vahid Mahdavi · Mahdieh Mardani

Received: 11 October 2014 / Accepted: 27 January 2015 / Published online: 15 February 2015

Abstract In this work, SBA-15 molecular sieves were functionalized with propylamine. A series of Mn(Salen)Cl complexes immobilized on amine functionalized SBA-15 (SBA-15-pr-NH_2) with different loading of Mn in range of 0.293–0.765 mmol Mn/g catalyst were prepared. These samples were characterized by BET, XRD, TGA–DSC, UV–Vis and FT-IR. The catalytic activity of immobilized Mn(Salen)Cl complexes was evaluated in the oxidation of benzyl alcohol in the liquid phase using *tert*-butylhydroperoxide (TBHP) as the oxidant. It was found that Mn(Salen) complexes immobilized on the SBA-15-pr-NH_2 are an efficient catalyst for the oxidation of benzyl alcohol and showed high catalytic activity and selectivity to benzaldehyde. As we expected, the leaching of manganese complexes from the support during the reaction was negligible, because of strong interaction between Mn(Salen)Cl complexes and the amine groups on the surface. The effects of Mn loading and various solvents on the conversion and selectivity were studied. A second order function for the variation in catalytic activity with respect to the loading of Mn(Salen)Cl in different catalyst samples was observed. The activity of the SBA-15-pr-Mn(Salen)Cl catalyst differs with the type of the solvent, and, in this case, acetonitrile gives the best conversion results. The influences of reaction temperature, reaction time, solvent, reusability, amount of catalyst and TBHP to benzyl alcohol molar ratio were investigated. Under optimized conditions, 73.5 % conversion of benzyl alcohol and 100 % selectivity to benzaldehyde was achieved.

Keywords Mn(Salen)Cl · Amine-functionalized SBA-15 · Mesoporous catalysts · Selective oxidation · Benzyl alcohol · Oxidation of alcohols

V. Mahdavi (✉) · M. Mardani
Surface Chemistry and Catalysis Division, Department of Chemistry, Faculty of Sciences, Arak University, 38156-8-8349 Arak, Iran
e-mail: v-mahdavi@araku.ac.ir

Introduction

Selective oxidation of alcohols to aldehydes, in particular benzyl alcohol to benzaldehyde, is an important organic transformation. Benzaldehyde is a very valuable chemical which has widespread applications in perfumery, dyestuff and agrochemical industries [1, 2]. Catalytic oxidation of benzyl alcohol (BzOH) to benzaldehyde (BzH) has attracted much attention both in the laboratory and in the chemical industry [3–8]. Vapor phase oxidation of benzyl alcohol to benzaldehyde has been extensively investigated in the past [9–14]. However, in the vapor phase oxidation process, it is not possible to avoid the total oxidation of part a of the benzyl alcohol to carbon oxides, thus causing a very significant carbon loss. The carbon loss can be avoided by carrying out the catalytic oxidation of benzyl alcohol in a liquid phase at temperatures lower than that used in the vapor phase oxidation process. Several studies have been reported on the catalytic oxidation of BzOH to BzH with different catalysts and oxidants in the liquid phase [15–20]. The increasing needs of efficient and selective catalysts as well as the fundamental investigations are the continuing driving forces for the synthesis of new materials.

Metal Schiff base complexes have been extensively studied as homogeneous catalysts for various oxidation reactions. Recently, some metal Schiff base complexes have been immobilized onto MCM-41, and the heterogenized metal complexes can increase catalyst stability and allow for catalyst recycling and product separation [21–23]. However, compared to the MCM-41 support, SBA-15 usually possesses wider pores, high pore volumes and thicker pore walls, which are more suitable for use in aqueous media. Moreover, some amino-modified SBA-15 hybrid materials have been successfully prepared [24] and further used for the immobilization of metal complexes [25].

The ability of a silica surface for amine functionalizing is determined by the content of different types of silanol groups, Si–OH. Kozlova and Kirik [26] determined the silanol density to be in the range of 3–4 OH/nm^2 for MCM-41 samples and 5–6 OH/nm^2 for SBA-15. Therefore, we expect that metal complexes immobilized on SBA-15-pr-NH_2 have higher catalytic activity compared to the MCM-14-supported one. SBA-15-pr-NH_2 have higher amine group contents on the surface and larger pore size which increase the ability of metal loading on the surface and facilitate reactant diffusion.

In the past, we have reported [27] the preparation of Mn(II) 2,2-bipyridine complexes immobilized over mesoporous hexagonal molecular sieves (HMS) and their application for selective oxidation of benzyl alcohol with *tert*-butyl hydroperoxide in the liquid phase.

In this paper, we used 3-aminopropyltrimethoxysilane (APTMS) to modify the mesoporous material SBA-15 to form the –NH_2 group on the support. The objectives of the present investigation were to prepare and characterize the Mn(Salen)Cl complexes covalently anchored onto the surface of SBA-15 functionalized with amine, and its application as an efficient and recyclable catalyst for liquid phase oxidation of benzyl alcohol in the presence of *tert*-butyl hydroperoxide (TBHP) as the oxidant.

In order to study the structure of the Mn(Salen) complexes supported on SBA-15, we have carried out characterization by XRD, N_2 physisorption, SEM, TGA, DSC, diffuse reflectance UV–Vis and FT-IR spectroscopy. The immediate goals of our study are the investigation of the relationship between structure and catalytic performance, and the effect of the Mn loading and solvents on the catalytic activity. Also, the effects of reaction time, oxidant/alcohol molar ratio, temperature, the amount of catalyst, catalyst recycling and leaching were investigated.

Experimental

Materials

All reagents used in the experiment, benzyl alcohol (BzOH), *tert*-butylhydroperoxide (TBHP) 75 % solution in water, acetonitrile, dioxane, toluene, *n*-Hexane, THF, chloroform, and ethanol were of the highest commercial quality and purchased from Aldrich and Merck and used without further purification.

The raw materials used in the synthesis of SBA-15 samples were tetraethyl orthosilicate (TEOS; 98 % Merck) as the silica source, poly(ethyleneglycol)-block-poly(propyleneglycol)-block-poly(ethyleneglycol) (;pluronic P123, $EO_{20}PO_{70}EO_{20}$, average molecular weight = 5,800; BASF) as the template, glycerol, hydrochloric acid (HCl, 1 N) as the pH controlling agent, and ethanol. Mn(Salen)Cl, where salen = *N*,*N*′-ethylenebis(salicylidenaminato), was also prepared according to previous work [28]. 3-Aminopropyltrimethoxysilane (APTMS) was purchased from Aldrich.

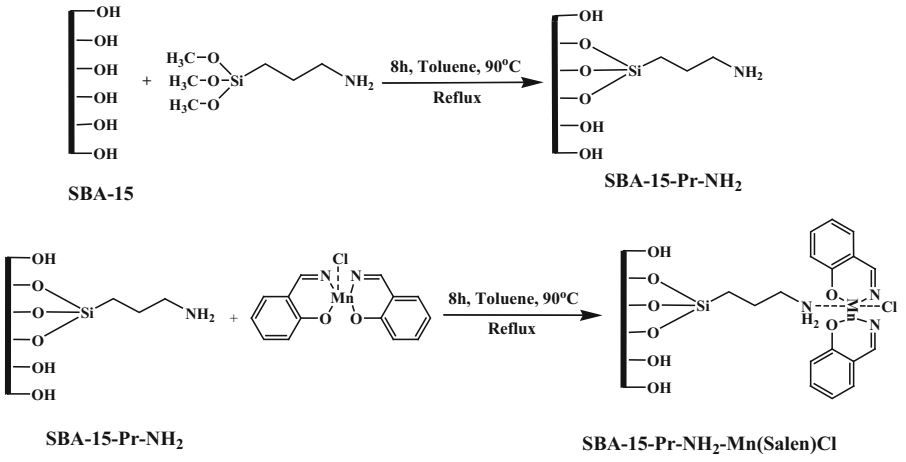

Fig. 1 Preparation of SBA-15-pr-NH_2-supported Mn-salen complexes

Preparation of catalysts

Synthesis of SBA-15

A typical procedure of synthesis according to the literature [29] is described below. Amounts of 1.8 g of P123 and 1.8 g of glycerol were dissolved in 69 g aqueous acidic solution with an HCl concentration of 1 M, which was stirred at 35 °C for 6–10 h to get a transparent solution. Then, 3.87 g of TEOS was added to the above solution under vigorous stirring. After stirring for 5 min, the mixture was kept in static conditions at the same temperature for 24 h, followed by aging at 100 °C for 24 h. The solid products were collected by filtration, washed with water, and dried at 80 °C overnight in air. The resulting powders were calcined at 550 °C for 5 h to remove the surfactant.

Synthesis of amine-functionalized SBA-15 (SBA-15-pr-NH_2)

Amine functionalization was accomplished by condensation of APTMS with the surface silanol groups of SBA-15 (Fig. 1) [30, 31]. In a typical synthesis, 4 g of calcined SBA-15 was first activated under vacuum at 150 °C for 4 h. It was then dispersed in 100 mL of dry toluene taken in a double-necked round-bottom flask (250 mL) fitted with a water-cooled condenser. Subsequently, an appropriate amount of APTMS dissolved in anhydrous toluene was added dropwise to the above suspension. The contents of the flask were refluxed for 24 h in nitrogen. The resulting mixture was cooled, filtered, washed with anhydrous toluene, dried at room temperature overnight and Soxhlet extracted, initially with toluene (overnight) and then with dichloromethane (for 6 h). The amine-functionalized SBA-15 (hereafter referred to as SBA-15-pr-NH_2) thus obtained was dried at 353 K for 6 h and used in further preparations.

Preparation of immobilized Mn(Salen)Cl complexes

The Mn(Salen) complexes immobilized on SBA-15 functionalized with amine (see Fig. 1) were synthesized as follows. The amine-functionalized SBA-15 (SBA-15-pr-NH_2) was first activated at 80 °C under vacuum for 2 h, and then dispersed in 50 mL of dry toluene. An appropriate amount of neat Mn(Salen)Cl was added and the contents of the flask were refluxed under nitrogen atmosphere for 24 h. The solid was filtered, dried at 60 °C and Soxhlet-extracted, initially with toluene for 12 h and then with dichloromethane for another 12 h. The light brown solid Mn catalyst material [SBA-15-pr-NH_2-Mn(Salen)Cl] thus prepared, dried (80 °C, 12 h), and used further in characterization and catalytic activity studies.

The final sample denoted as SBA-15-pr-NH_2-Mn(Salen)(x), where x represents the final Mn content (mmol Mn/g catalyst) in the sample tested by atomic absorption spectroscopy.

Catalyst characterization

The surface areas of SBA-15-pr-NH_2-Mn(Salen)Cl samples were measured using the Brunauer–Emmet–Teller (BET) method on a Micromeritics ASAP 2010 instrument using N_2 as the adsorbent. The structure of these samples was studied by X-ray diffraction (XRD) experiments. A Philips model PW 1800 diffractometer with Cu-Kα radiation and a Ni filter was used to collect the X-ray data. The contents of manganese in the samples were determined by atomic absorption spectroscopy (AAS) using a Perkin-Elmer Analyst instrument, after extraction of Mn from the catalyst samples in HNO3 and HF acids.

The analyses of C, H and N elements were obtained with a VarioEL II analyzer. Thermal stability of samples was studied with thermogravimetric and differential scanning calorimetry (TG–DSC) using a PL-1500 instrument. Nitrogen gas was used as carrier gas for TGA experiment and the flow rate of N_2 was about 40 mL/min. The heating rate was set at 10 °C/min with scans from ambient temperature to 800 °C. The scanning electron microscopy (SEM) images were obtained with a Philips XL30 instrument. The infrared spectra of the catalysts were taken as KBr pellets on a Galaxy-5000 Fourier transform IR (FT-IR). A JASCO V-670 Spectrophotometer was used to collect the diffuse reflectance UV–Vis spectra data. The spectra were collected in the range of 200–900 nm at room temperature with $BaSO_4$ as the reference.

Oxidation of benzyl alcohol

In a typical procedure, a mixture of 0.1 g SBA-15-pr-NH_2-Mn(Salen)Cl catalyst with the grain size of 200–230 mesh, 15 mL solvent (acetonitrile) and 10 mmol of benzyl alcohol was stirred in a three-necked flask under nitrogen atmosphere at 50 °C for 30 min. The stirring rate of the solution was set at 750 cycle/min. Then, 10 mmol of the oxidant (TBHP) was added to the solution and the mixture was refluxed for 8 h under nitrogen atmosphere. After filtration, the reaction mixture was analyzed by GC. A GC–MS of model Thermo Finnigan (60 m, RTX-1 column) was used for the identification of products and a GC (Perkin Elmer Model 1800) was used for the product analysis. The GC was equipped with a flame ionization detector (FID) connected to a 3 % OV-17 column with length of 2.5 m and diameter of 1/8 in.

Results and discussion

Catalyst characterization

The nitrogen adsorption–desorption isotherms and the corresponding pore size distributions of SBA-15 and SBA-15-pr-NH_2-Mn(Salen)(0.512) samples are shown in Fig. 2. These isotherms correspond to type IV with a broad H1-type hysteresis that is typical of mesoporous materials with 1-D cylindrical channels. The adsorption branches were located at relative pressures in the range from 0.4 to 0.8.

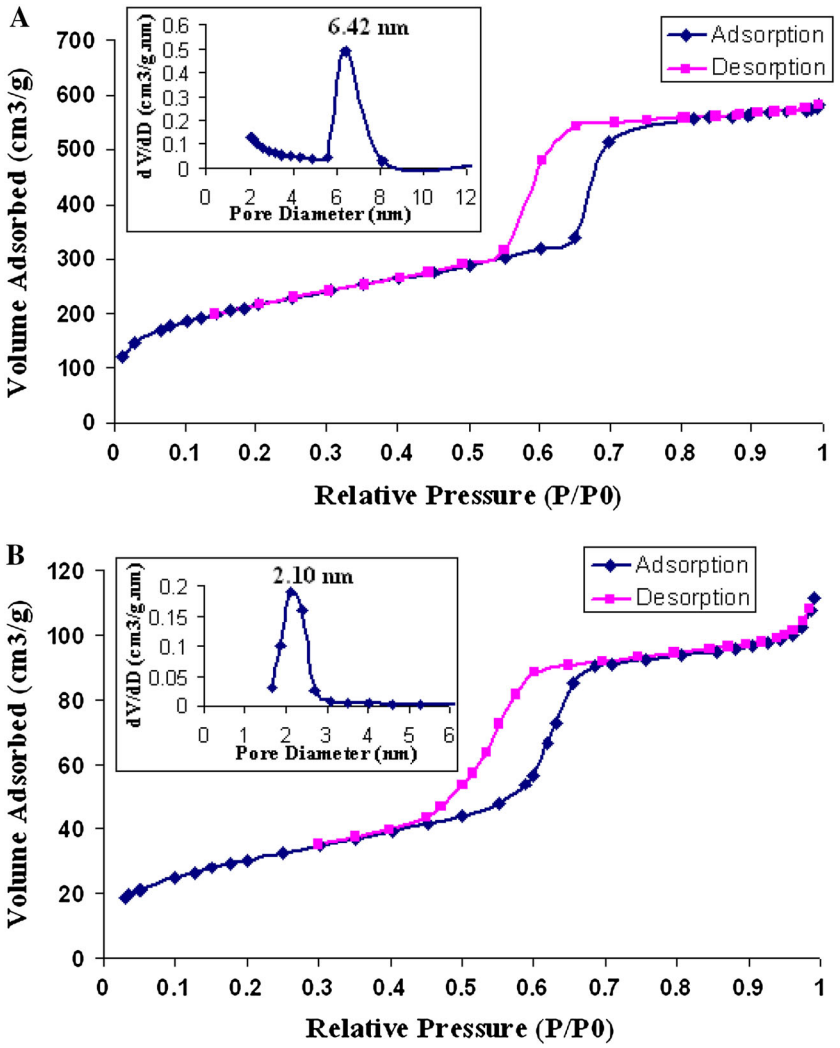

Fig. 2 N_2 adsorption/desorption isotherms and BJH analysis for **a** SBA-15, and **b** SBA-15-pr-NH_2-Mn(Salen)(0.512) samples

These results confirm the typical mesoporous structures of SBA-15-pr-NH_2-Mn(Salen)Cl samples. The BET surface area values pore diameters and pore volumes of all catalysts are given in Table 1. As shown in Table 1, the average pore diameter for the Mn(Salen) complex immobilized on SBA-15 catalysts compared to SBA-15 do not differ that much, and there is a significant decrease in the pore volume and surface area of the Mn(Salen) complex immobilized on SBA-15 catalysts. This change in the surface area is as one would expect. By immobilizing the Mn(Salen) complex onto the support, the surface of the support on which nitrogen can adsorb becomes less and causes the decrease in the total volume of

Table 1 Chemical composition and physical properties of the immobilized Mn(Salen)Cl complex on the SBA-15-pr-NH_2 support

Sample	Chemical composition (wt%)				Mn loading (mmol Mn/g catalyst)	S_{BET} (m^2/g)	Total pore volume (cm^3/g)	Average pore diameter (Å)
	C	H	N	Mn				
SBA-15	–	–	–	–	–	781	0.91	45.4
SBA-15-pr-NH_2	10.90	2.80	3.60	–	–	670	0.83	43.2
SBA-15-pr-NH_2-Mn(Salen) (0.293)	15.18	2.91	4.05	1.61	0.293	490	0.46	42.8
SBA-15-pr-NH_2-Mn(Salen) (0.366)	16.23	2.95	4.15	2.01	0.366	370	0.34	41.6
SBA-15-pr-NH_2-Mn(Salen) (0.440)	17.46	2.98	4.27	2.43	0.440	256	0.27	42.4
SBA-15-pr-NH_2-Mn(Salen) (0.512)	18.53	2.99	4.37	2.81	0.512	112	0.17	41.2
SBA-15-pr-NH_2-Mn(Salen) (0.647)	20.63	3.06	4.58	3.55	0.647	92	0.11	40.7
SBA-15-pr-NH_2-Mn(Salen) (0.765)	22.45	3.11	4.76	4.20	0.765	85	0.04	41.6
Neat Mn(Salen)Cl	53.86	3.93	7.85	15.42	–	–	–	–

nitrogen that can be adsorbed. The expected decrease in the surface area was observed for these samples showing that immobilization of the Mn(Salen) complex were successful.

The amount of the NH_2 functional group and the immobilized Mn(Salen)Cl complex in different catalysts estimated by chemical analyses are listed in Table 1. Mn(Salen)Cl could be immobilized directly on "bare" SBA-15. However, the amount immobilized was very low (0.07 mmol/g catalyst) compared to that on the amine-functionalized surfaces (0.293, 0.366, 0.440, 0.512, 0.647, 0.765 mmol/g catalyst) in the SBA-15-pr-NH_2-Mn(Salen)Cl. The complex immobilized directly on the pristine SBA-15 surface was leached out completely during the oxidation reactions.

The low-angle XRD patterns of the SBA-15, SBA-15-pr-NH_2 and manganese Salen complex-immobilized SBA-15-pr-NH_2 samples are shown in Fig. 3. The SBA-15 support shows three peaks at 2θ of 0.5°–3°, corresponding to the diffraction of (100), (110), and (200) planes. These peaks are characteristic of the hexagonally ordered structure of SBA-15. The hexagonal array gives a rather broad and poorly defined X-ray diffraction pattern, and low angles ($\theta < 1°$) are necessary to observe the (100) reflection, which is usually the strongest peak. This in itself is an indication that large features have been created because the Bragg equation shows that the d_{100} interlattice spacing is more than 4.4 nm when θ is less than 1°.

The Mn(Salen) complex immobilized samples showed the same pattern, indicating that the long-range order of the SBA-15 framework was well retained after the grafting process, although the intensity of these diffraction peaks was decreased. The decrease in peak intensity suggests the irregular organization at

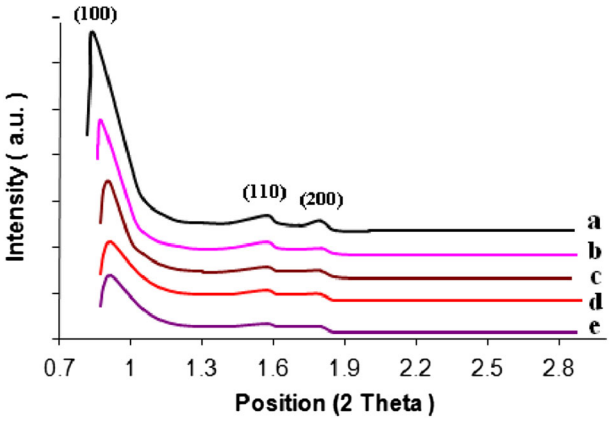

Fig. 3 Low-angle XRD patterns of *a* SBA-15, *b* SBA-15-pr-NH_2, *c* SBA-15-pr-NH_2-Mn(Salen)(0.366), *d* SBA-15-pr-NH_2-Mn(Salen)(0.512), *e* SBA-15-pr-NH_2-Mn(Salen)(0.647)

long-range order of the mesoporous structure, arising from the organo-functionalization of SBA-15 mesopores.

The SEM images of SBA-15-pr-NH_2, SBA-15-pr-NH_2-Mn(Salen)(0.293) and SBA-15-pr-NH_2-Mn(Salen)(0.512) samples with two magnificationd are shown in Fig. 4a–f. SEM micrographs of SBA-15-pr-NH_2 clearly show agglomerate particles with rod-like morphology which are in agreement with the results observed in XRD tests and the average length and width were ca. 2.6 and 0.53 μm, respectively.

In addition, the SEM image (Fig. 4) of the catalysts indicated that agglomerated manganese complexes particles, with particle size around 80–90 nm, were well deposited on the surface of SBA-15 and some of them were distributed within the SBA-15 mesoporous but the uniformity of the size of the rod like particles gets reduced after the immobilizing of Mn(Salen)Cl complex on the surface pore wall of the SBA-15.

The FT-IR spectra of neat Mn(Salen)Cl complex, SBA-15-pr-NH_2 and the immobilized sample SBA-15-pr-NH_2-Mn(Salen)(0.512) are shown in Fig. 5.

A broad band was observed for SBA-15-pr-NH_2 in the hydroxyl range, 4,000–3,000 cm^{-1}, that was assigned to isolated silanol groups and adsorbed water on the surface of the solid. A peak at 1,558 cm^{-1} was observed for SBA-15-pr-NH_2 due to the N–H bonds in the amine group and 2,765 and 2,560 cm^{-1} due to C–H stretching modes of the propyl spacer (Fig. 5). Additionally, there are three typical peaks for SBA-15-pr-NH_2 in the Si–OX stretching range as follows: $\upsilon OH(H_2O)$ 2,900–3,400 cm^{-1}, $\delta OH(H_2O)$ 1,660 cm^{-1}, υ_{as}(Si–O–Si) 1,107 cm^{-1}, δOH (Si–OH) 945 cm^{-1}, υ_s(Si–O–Si) 800 cm^{-1}, and δ(Si–O–Si) 465 cm^{-1}. Two of the three bands are related to the intrinsic vibrations, symmetric υ_s(Si–O–Si) and asymmetric υ_{as}(Si–O–Si), of the tetrahedral unit $SiO4^{4-}$ (at 800 and 1,107 cm^{-1}, respectively, for SBA-15-pr-NH_2) and the other one is assigned to the stretching vibration, δOH(Si–OH), of the Si–O moiety of the silanol groups Si–O···H on the

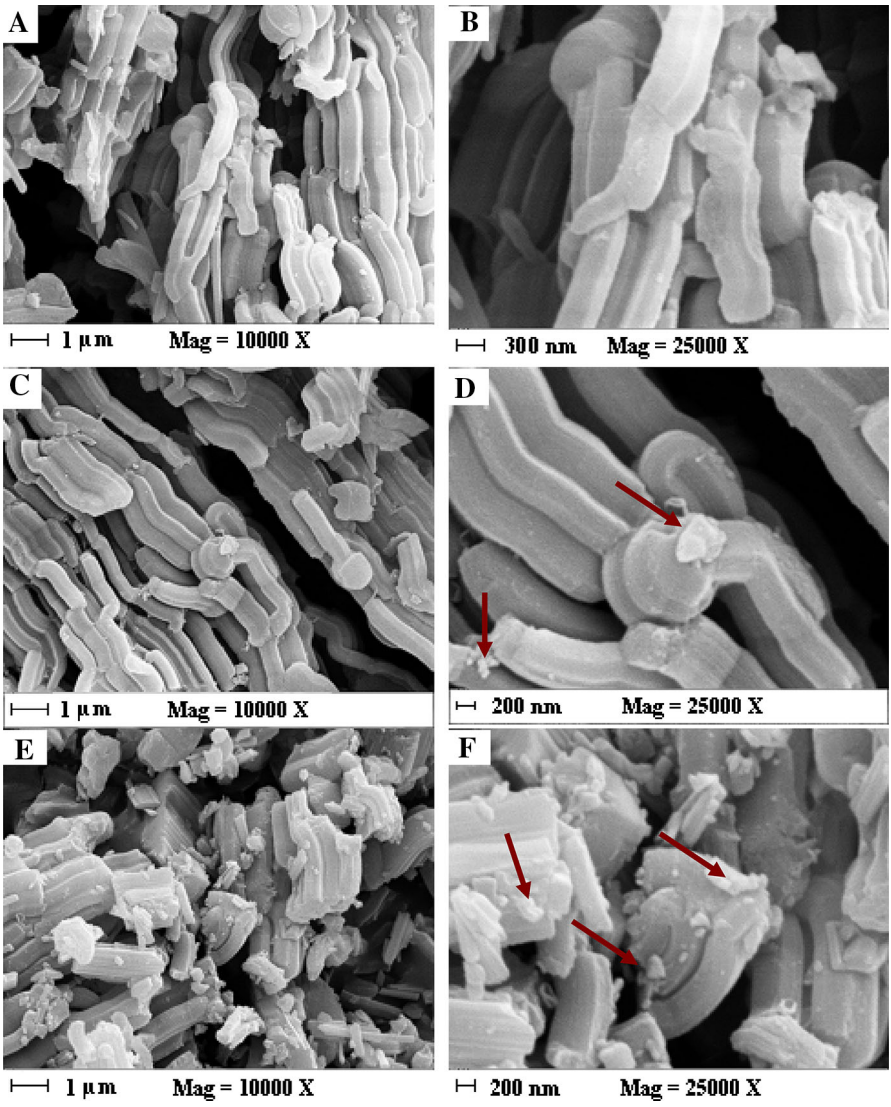

Fig. 4 Scanning electron micrographs (SEM) of **a**, **b** SBA-15-pr-NH_2, **c**, **d** SBA-15-pr-NH_2-Mn(Salen)(0.0.293), and **e**, **f** SBA-15-pr-NH_2-Mn(Salen)(0.512) samples at two different magnifications

surface (at 945 cm^{-1} for SBA-15-pr-NH_2). There is one additional peak at the low wave number that corresponds to the skeletal deformation of the same tetrahedral unit $SiO4^{4-}$, δ(Si–O–Si) at 465 cm^{-1}.

The FT-IR spectra of neat Mn(Salen)Cl complex and the immobilized sample SBA-15-pr-NH_2-Mn(Salen)(0.512) are shown in Fig. 5. The peaks due to the azomethine group υ(C=N) of the Salen Schiff base ligand shifted from 1,628 and 1,599 cm^{-1} for the "neat" Mn-complex [32] to 1,630 and 1,605 cm^{-1} for the

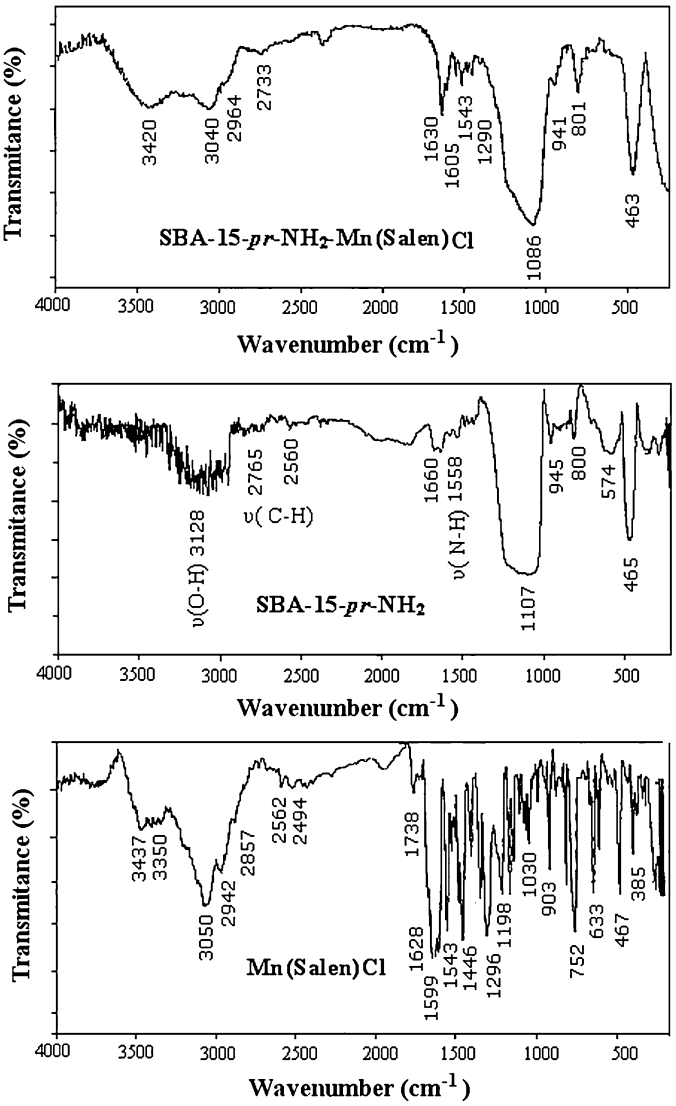

Fig. 5 FT-IR spectra of neat Mn(Salen)Cl complex, SBA-15-pr-NH_2 and SBA-15-pr-NH_2-Mn(Salen)(0.512)

immobilized Mn(Salen) complex. Similarly, the peak due to υ(C–O) shifted from 1,296 cm^{-1} for the neat complex [32] to 1,290 cm^{-1} for the immobilized Mn-complex. The data of FT-IR for these samples is shown in Table 2.

The diffuse reflectance UV–Vis spectra of SBA-15, SBA-15-pr-NH2, SBA-15-pr-NH_2-Mn(Salen)(0.512) and neat Mn(Salen)Cl samples are shown in Fig. 6. The UV–Vis spectra of SBA-15 contains the peaks at about 249 and 286 nm which could be assigned to tetrahedral oxygen-coordinated Si ions. Mn(III)Salen

Table 2 FT-IR frequencies of the immobilized Mn(Salen)Cl complex on the SBA-15-pr-NH_2 support

Sample	From propyl amine		From Mn(Salen)Cl complex			
	υ(C–H) (cm^{-1})	υ(N–H) (cm^{-1})	υ(C=N) (cm^{-1})	υ(C=C) (cm^{-1})	Ring (cm^{-1})	υ(C–O) (cm^{-1})
SBA-15-pr-NH_2	2,765 2,560	1,558	–	–	–	–
Mn(Salen)Cl	–	–	1,628 1,599	1,543	1,446, 1,387 752	1,296
SBA-15-pr-NH_2-Mn(Salen)Cl	–	1,547	1,630 1,605	1,543	1,446, 1,380 754	1,290

complexes show bands near 254, 283 and 306 nm which could be assigned to π–π^* transition of the benzene ring of Salen, n–π^* transition of the C=N bond respectively [33]. In addition, bands of metal to ligand charge transfer (MLCT) at 390 nm and *d*–*d* transition at 465 nm is shown [34]. Typically, neat Mn(Salen)Cl showed weakly intense *d*–*d* transition bands at 420, 460, 564 and 723 nm [34]. These bands for Mn(Salen)Cl immobilized on propylamine-functionalized SBA-15 appeared at 493 and 570 nm.

The blue shift absorption between 200 and 470 nm in the case of SBA-15-pr-NH_2-Mn(Salen)(0.512) compared to neat Mn(Salen)Cl complex clearly shows the strong coordination of neat metal complex over amino-functionalized SBA-15.

FT-IR and diffuse reflectance UV–Vis results briefly indicate that immobilized samples of the manganese Salen complex have been successfully synthesized over the surfaces of SBA-15-pr-NH_2 and the Schiff base Salen ligand is not decomposed upon coordination to the organo-functional groups.

From FT-IR and DRUV–Vis studies, it has been found that immobilization of Mn(Salen)Cl has modified the geometry and electronic structure of the immobilized Mn-complex. Neat Mn(Salen)Cl in the crystalline state or in solution is consistent with the +3 oxidation state of the Mn ions. However, the solid immobilized Mn-complex shows a distinct redox couple in the cyclic voltammogram attributable to Mn^{4+}/Mn^{3+} [35].

Figure 7 shows TGA–DSC results for the SBA-15-pr-NH_2-Mn(Salen)(0.512) sample. The thermal analysis occurs in the two steps and shows one DSC peak. Step. 1 (endothermic), in the ranges of 25–372 °C, is involved with the water loss and the dehydroxylation of the SBA-15 surface (13.42 % weight loss of the sample). In the second step (exothermic), between 372 and 653 °C, the ligand groups of the SBA-15-pr-NH_2-Mn(Salen) sample are decomposed, and CO, CO_2 and NO_x gases perhaps are released (17.70 %, weight loss of the sample). Therefore, the total weight loss of the sample is 31.12 % and the results of TGA indicate that the Mn(Salen) complex-immobilized SBA-15-pr-NH_2 sample is thermally stable in the reaction temperature range of 27–90 °C.

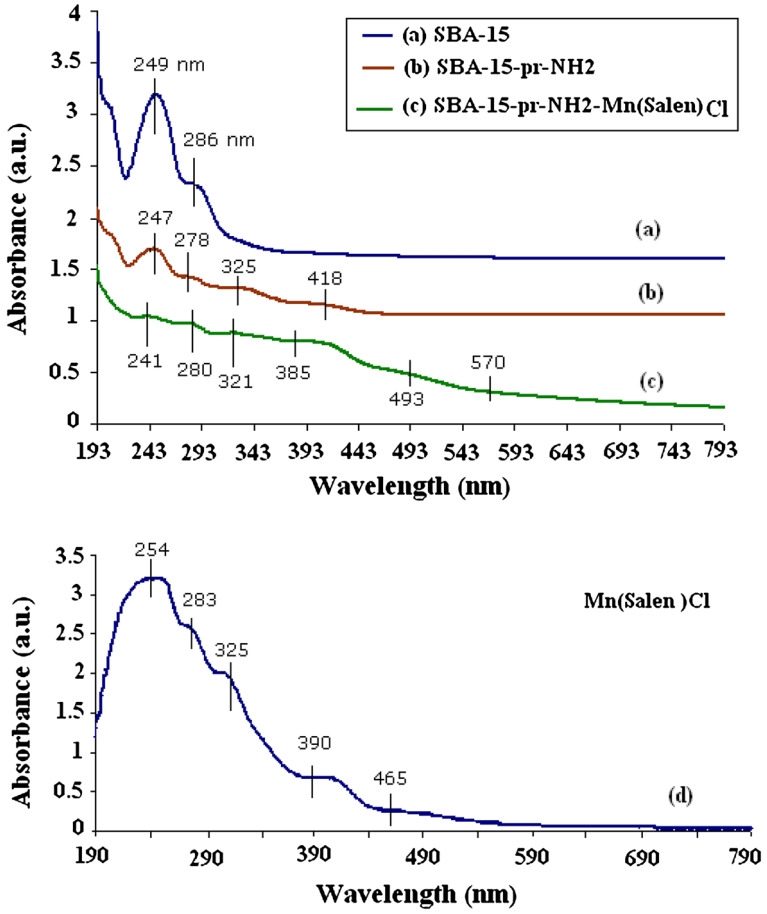

Fig. 6 Diffuse reflectance UV–VIS spectra of the *a* SBA-15 and *b* SBA-15-pr-NH_2 *c* SBA-15-pr-NH_2-Mn(Salen)(0.512) and *d* neat Mn(Salen)Cl complex

Oxidation of benzyl alcohol with TBHP on the SBA-15-pr-NH_2-Mn(Salen) catalysts

Oxidation of benzyl alcohol was studied exclusively for loading effect, solvent effect, effects of temperature, amount of catalyst, TBHP/benzyl alcohol molar ratio, recycling and leaching, and the results of the study are as follows.

Effect of loading of Mn(Salen)Cl complex on the activity of catalysts

The results of the oxidation of benzyl alcohol in the presence of TBHP and without a catalyst, SBA-15-pr NH_2 and SBA-15-pr-NH_2-Mn(Salen) samples with loading of 0.293, 0.366, 0.44, 0.512 and 0.647 and 0.765 mmol Mn/1 g catalyst, are shown in Table 3. All reactions were conducted at reflux temperature (90 °C) for 8 h with

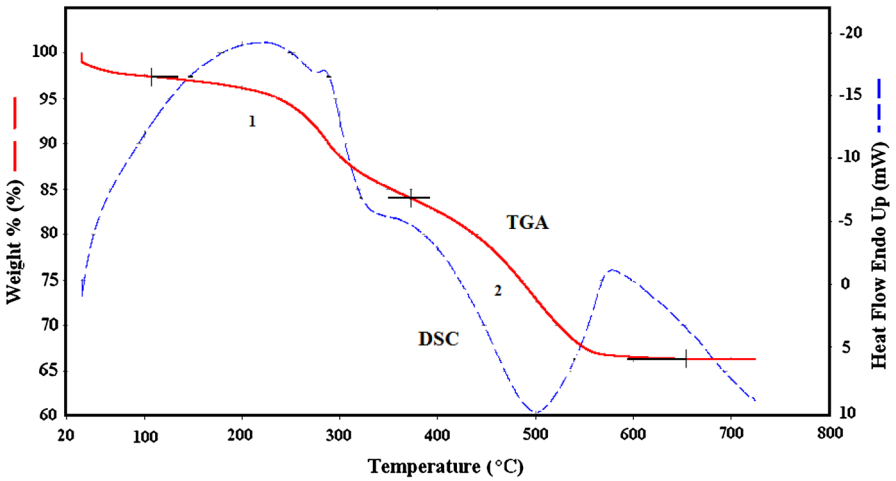

Fig. 7 Thermogravimetry and differential scanning calorimetry diagram of SBA-15-pr-NH_2-Mn(Salen)(0.512) sample. Step *1* (endothermic), in the range of 25–372 °C, elimination of humidity and the dehydroxylation of the SBA-15 surface; step *2* (exothermic), in the range of 372–653 °C, elimination of the ligand groups of SBA-15-pr-NH_2-Mn(Salen) sample

0.1 g of the catalyst, 15 mL solvent, acetonitrile, 10 mmol of the benzyl alcohol and 10 mmol TBHP. In all the reactions, the conversion percentage was calculated with respect to the substrate (benzyl alcohol). In the absence of any catalyst, benzyl alcohol conversion is lower than 5.4 %. SBA-15-pr NH_2 gives a benzyl alcohol conversion around 12.1 %. The result shows that the reactions with SBA-15-pr-NH_2-Mn(Salen) catalysts have relatively high conversion percentage compared to the SBA-15-pr NH_2 sample or blank reaction. In addition, the SBA-15-pr-NH_2-Mn(Salen)(0.512) catalyst has a higher conversion percentage (73.49 %) with respect to the other samples with 0.293, 0.366, 0.44, 0.647 and 0.765 mmol Mn/1 g catalyst. Table 3 shows that the selectivity of all catalysts is independent of the loading of Mn and, with increasing the loading of Mn(Salen)Cl on the SBA-15-pr NH_2, the selectivity with respect to benzaldehyde remains constant.

The data from Table 3 are used to plot Fig. 8 in which the variation of activity with respect to the loading of Mn in catalysts is shown. A second order function for the variation in catalytic activity with respect to the loading of Mn in different catalyst samples was observed as follows:

$$Y = -2.8065X^2 + 2.797X + 0.1438 \quad (1)$$

where X stands for loading of Mn and Y is the activity of catalyst sample.

In fact, these samples were active in this reaction, and their activities were basically proportional to their Mn loadings. But there was a restriction effect on the diffusion of the substrate and product through the channels of the solid. Moreover, this mass transfer resistance gradually increased with the Mn-complex loadings inside the support, which was confirmed from the data of turnover frequency listed in Table 3.

Table 3 Oxidation of benzyl alcohol with TBHP in the presence of SBA-15-pr-NH_2-Mn(Salen)catalysts

Entry	Catalyst	Mn loading[a] (mmol Mn/g catalyst)	Conversion[b] (%)	TOF[c] (h^{-1})	Selectivity[d] of benzaldehyde (%)
1	–	0	5.40[e]	–	100
2	SBA-15-pr-NH_2	0	12.10	–	100
3	SBA-15-pr-NH_2-Mn(Salen) (0.293)	0.293	50.82	21.68	100
4	SBA-15-pr-NH_2-Mn(Salen) (0.366)	0.366	57.64	19.69	100
5	SBA-15-pr-NH_2-Mn(Salen) (0.440)	0.440	61.39	17.44	100
6	SBA-15-pr-NH_2-Mn(Salen) (0.512)	0.512	73.49	17.94	100
7	SBA-15-pr-NH_2-Mn(Salen) (0.647)	0.647	54.93	10.61	100
8	SBA-15-pr-NH_2-Mn(Salen) (0.765)	0.765	48.06	7.85	100

Reaction condition: 0.1 g catalyst with the grain size of 200–230 mesh; benzyl alcohol 10 mmol; TBHP 10 mmol; 15 mL acetonitrile; reflux temperature(90 °C); reaction time 8 h, the stirring rate of the reaction mixture 750 cycles/min

[a] The contents of Mn were determined by AAS

[b] Conversion = (moles of benzyl alcohol reacted/moles of benzyl alcohol in the feed) × 100

[c] Turnover frequency (TOF) was calculated from benzyl alcohol amount (mmol) × its conversion (%)/(catalyst amount (g) × Mn loading (mmol g^{-1}) × reaction time (h))

[d] Selectivity = (moles of benzyl alcohol converted to benzaldehyde/moles of alcohol reacted) × 100

[e] Without catalyst

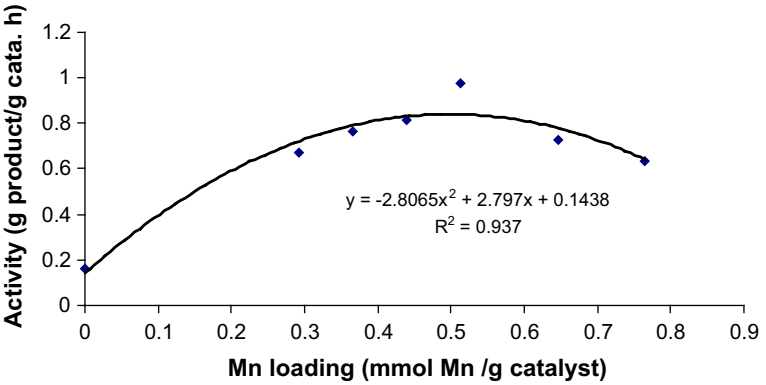

Fig. 8 Activity of SBA-15-pr-NH_2-Mn(Salen) catalyst as a function of Mn loading. Reaction condition: 0.1 g SBA-15-pr-NH_2-Mn(Salen) catalyst with the grain size of 200–230 mesh; benzyl alcohol 10 mmol; TBHP 10 mmol; 15 mL acetonitrile; reflux temperature (90 °C); reaction time 8 h, the stirring rate of the reaction mixture 750 cycles/min

Table 4 Benzyl alcohol oxidation using various heterogeneous catalysts

Catalyst	Oxidant	Time (h)	Benzyl alcohol conversion (%)	Selectivity of aldehyde (%)	References
SBA-15-pr-NH_2-Mn(Salen)(0.512)	TBHP	8	73.49	100	Our catalyst
$[Mn(bpy)_2]^{2+}$/HMS	TBHP	8	49.2	100	[27]
(V2O5/OMS-2)	TBHP	8	79.9	100	[36]
Cr(Salen)-NH_2-MCM-41	H_2O_2	4	52.5	100	[37]
$(PPh_4)_2[Mn(N)(CN)_4]$	H_2O_2	1	70	25	[38]
Mn/SiO_2	O_2	4	63	99	[39]
Mn–Cr–HT	O_2	–	18.7	99.5	[15]
Mn_3O_4 nanoparticles	O_2	8	65	–	[40]
Mn–Cr–LDH	TBHP	5	49.8	83.5	[41]

HT hydrotalcite like solid catalyst, *LDH* layered double hydroxides

On the SBA-15-pr-NH_2-Mn(Salen)(0.512) catalyst, the conversion of benzyl alcohol was 73.49 % and the selectivity of benzaldehyde was 100 %. Therefore, this sample may be a better catalyst with respect to the all other catalysts listed in Table 3.

The oxidation of benzyl alcohol with TBHP and O_2 over the various tested catalytic systems is given in Table 4. In comparison with catalysts reported in our previous work [27, 36], the SBA-15-pr-NH_2-Mn(Salen)(0.512) catalyst was evaluated with a high level of activity, and it is seen that this catalyst has comparable catalytic activity with respect to other catalytic systems [15, 37–41]. Therefore, this catalytic system has been determined as suitable for the oxidation of benzyl alcohol

Effects of temperature and reaction time

In this experiment, the change in conversion (%) of benzyl alcohol in the presence of TBHP oxidant and SBA-15-pr-NH_2-Mn(Salen)(0.512) catalyst at 30, 50, 70 and 85 °C was monitored and plotted with respect to time (Fig. 9). The reaction was carried out with using 0.1 g catalyst, 15 mL acetonitrile, 10 mmol of TBHP and 10 mmol of benzyl alcohol in a three-necked round-bottom flask, and many samples were drawn out at regular intervals and analyzed by GC.

From Fig. 9, we can conclude that, as time increases, the conversion of benzyl alcohol increases continuously until 99 % without any inhibitory effect being observed in reaction system.

The effect of temperature on the reaction rate showed that the catalytic activity strongly increased with the increasing of the reaction temperature, and the selectivity toward benzaldehyde is constant. According to Fig. 9, the time for 45 % conversion of benzyl alcohol changed from 6 h at 50 °C to 3 h at 90 °C.

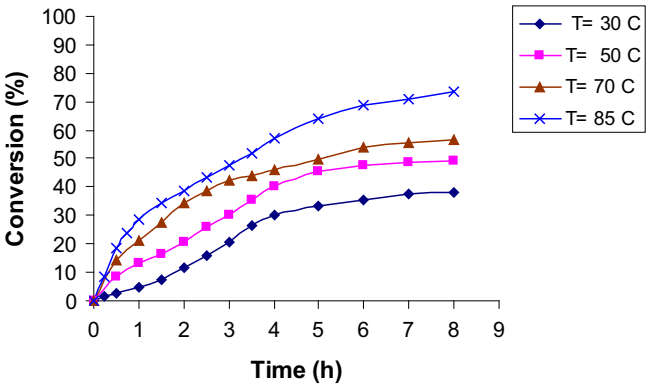

Fig. 9 Conversion of benzyl alcohol as a function of time at 30, 50, 70 and 85 °C in the presence of TBHP oxidant and SBA-15-pr-NH_2-Mn(Salen)(0.512) catalyst

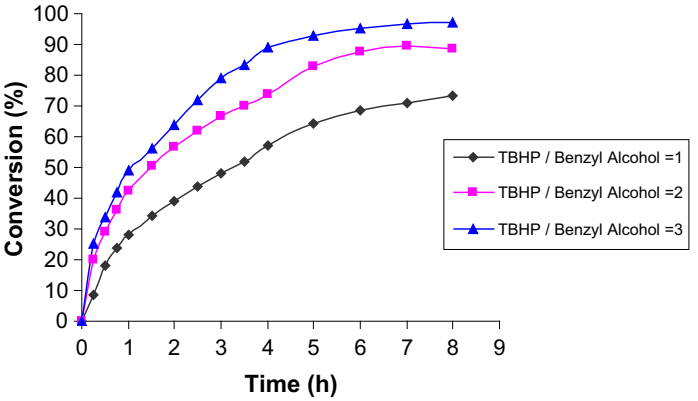

Fig. 10 Conversion of benzyl alcohol as a function of time at 1, 2 and 3 TBHP/benzyl alcohol molar ratio in the presence of SBA-15-pr-NH_2-Mn(Salen)(0.512) catalyst

Effect of oxidant/alcohol molar ratio

This experiment evaluated the change in the conversion (%) of benzyl alcohol in the presence of TBHP oxidant and SBA-15-pr-NH_2-Mn(Salen)(0.512) catalyst with 1, 2 and 3 TBHP/benzyl alcohol molar ratios (Fig. 10). The reaction was carried out at reflux temperature (90 °C) using 0.1 g of catalyst, 15 mL of acetonitrile and three different amounts of TBHP, i.e. 10, 20 and 30 mmol for a fixed amount of benzyl alcohol (10 mmol) and reaction time (8 h).

The conversion percentage increased according to an increment of TBHP to benzyl alcohol molar ratio. However, the selectivity of benzaldehyde decreased due to the consecutive reaction of the transformation of benzaldehyde to benzoic acid. The lowest TBHP/benzyl alcohol ratio resulted in 73.49 % conversion of benzyl alcohol and 100 % selectivity to benzaldehyde, and the highest TBHP/benzyl

Table 5 Effect of amount of SBA-15-pr-NH_2-Mn(Salen)(0.512) catalyst on benzyl alcohol oxidation with TBHP as oxidant

Entry	Amount of catalyst	Conversion of benzyl alcohol (%)	Selectivity of benzaldehyde (%)
1	0.02	43.46	100
2	0.05	55.38	100
3	0.1	73.49	100
4	0.15	65.23	100
5	0.2	61.87	100
6	0.25	52.84	100

Reaction condition: benzyl alcohol 10 mmol; TBHP 10 mmol; 15 mL acetonitrile; reflux temperature (90 °C); reaction time 8 h

alcohol ratio (3:1) produced 95.6 % conversion and 44 and 56 % selectivity to benzaldehyde and benzoic acid, respectively.

Figure 10 shows that the conversion of benzyl alcohol increased up to 95 % without any inhibitory effect.

Effect of the amount of catalyst

In these experiments, the amounts of SBA-15-pr-NH_2-Mn(Salen)(0.512) catalyst were varied from 0.05 to 0.3 g for reactions carried out at 90 °C for 8 h, with other reaction conditions remaining constant. The results (Table 5) clearly demonstrate that there is a general trend of increasing conversion of benzyl alcohol by increasing catalyst amounts. However, when the catalyst amount was increased to higher than 0.1 g, the conversion decreased.

Sheldon and Kochi [1] reported that the transition metals complexes, especially in organic solvent, often behave as catalysts at low concentration but as inhibitors at high concentration. This phenomenon is often referred to as catalyst-inhibitor conversion.

In fact, high amounts of catalyst may actually favor the homolytic decomposition of the TBHP, and the catalyst may compete effectively with the benzyl alcohol for the *t*-butyl peroxy radicals, which formed from the TBHP decomposition. Therefore, the efficiency of radicals toward oxidation may be lower at higher concentrations of radicals than at lower concentrations.

Effect of solvents

In these experiments, the solvent was changed for each run, while the other conditions, 0.1 g of the SBA-15-pr-NH_2-Mn(Salen)(0.512) catalyst, 15 mmol benzyl alcohol, 15 mmol TBHP, stirring rate of the reaction mixture 750 cycle/min and reaction temperature, 70 °C for 8 h, remained the same. The solvent has been varied from a polar to a nonpolar state. The results of the conversion of benzyl alcohol with the various solvents are shown in Table 6.

Table 6 Effect of solvents on oxidation of benzyl alcohol with TBHP in the presence of SBA-15-pr-NH_2 Mn(Salen)(0.512) catalyst

Solvent	Dielectric constant	Dipole moment (D)	Conversion (%)	Selectivity (%)
Acetonitrile	37.5	3.92	73.49	100
THF	7.5	3.89	34.41	100
Chloroform	4.8	1.15	21.46	100
Toluene	2.4	0.37	51.14	100
Dioxane	2.25	0.45	54.40	100
n-Hexane	–	–	39.32	100

Reaction condition: 0.1 g catalyst; benzyl alcohol 15 mmol; TBHP 15 mmol; solvent 7.5 mL; Reaction temperature 70 °C; reaction time 8 h

As demonstrated in Table 5, the behavior of benzyl alcohol oxidation in various solvents was strikingly different. The conversion (%) of benzyl alcohol decreased in the order: acetonitrile > dioxane > toluene > *n*-hexane > THF > chloroform with 100 % selectivity to benzaldehyde.

Acetonitrile is a polar solvent with a very high dielectric constant; it can readily dissolve TBHP along with the benzyl alcohol and increase the efficiency of the catalytic system. Also, highly polar solvents like acetonitrile may facilitate the formation of active oxygen species and thereby enhance the catalytic activity.

Metal-catalyzed oxidation involving alkyl peroxides may proceed either through a homolytic or a heterolytic mechanism. Transition metal salts of Co, Mn, Fe, Cu, or the metal oxides are normally involved in homolytic cleavage [1]. Therefore; we suggested that the oxidation pathway may be as follows:

$$MnL_2^n + t\text{-butOOH} \rightarrow t\text{-butO}^{\cdot} + MnL_2^nOH \quad (2)$$

$$MnL_2^n + t\text{-butOOH} \rightarrow t\text{-butOO}^{\cdot} + MnL_2^n + H^{\cdot} \quad (3)$$

$$t\text{-butOO}^{\cdot} + RCH_2{-}OH \rightarrow \text{t-butOOH} + RCH^{\cdot}{-}OH \quad (4)$$

$$t\text{-butO}^{\cdot} + RCH_2{-}OH \rightarrow \text{t-butOH} + RCH^{\cdot}{-}OH \quad (5)$$

$$RCH^{\cdot}{-}OH \rightarrow RCHO + H^{\cdot} \quad (6)$$

where RCH_2–OH = benzyl alcohol, RCHO = benzaldehyde

Catalyst recycling and leaching

The catalyst SBA-15-pr-NH_2 Mn(Salen)(0.512) was selected for tests and benzyl alcohol was used as a model substrate for evaluating recycling and leaching. Leaching of the catalyst was tested by filtering the catalyst during the reaction and checking the conversion progress in the filtrate solution. In this study, a mixture of 0.1 g catalyst SBA-15-pr-NH_2-Mn(Salen)(0.512), 7.5 mL acetonitrile, 15 mmol TBHP and 15 mmol of benzyl alcohol was refluxed for 4 h and a conversion of 53.59 % was obtained. Then, the reaction mixture was filtered and then the filtrate

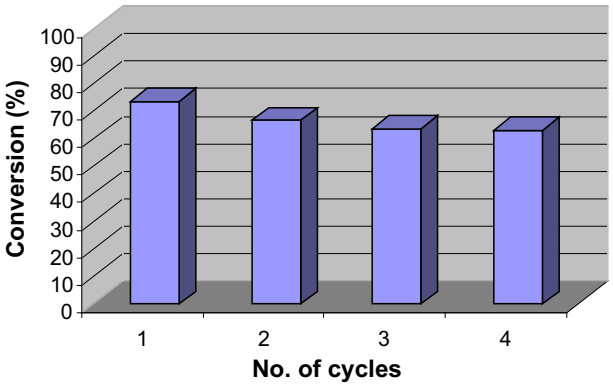

Fig. 11 The effect of catalyst recycling. Reaction condition: 0.1 g SBA-15-pr-NH_2-Mn(Salen)(0.512) catalyst; benzyl alcohol 10 mmol; TBHP 10 mmol; 15 mL acetonitrile; reflux temperature (85 °C); reaction time of a run 8 h

solution was refluxed for the next 4 h and the conversion level of 59.66 % was obtained. Therefore, only 6.07 % conversion was increased during the second 4 h. In comparison, another experiment was carried out by refluxing the initial reaction mixture for 8 h without catalyst filtration, producing a conversion level of 73.49 %. The result of the oxidation of benzyl alcohol in the presence of TBHP and without a catalyst is also shown in Table 3. In the absence of any catalyst, benzyl alcohol conversion is lower than 5.4 % for 8 h reaction time. The Mn content in the filtrate solution was analyzed by atomic absorption spectroscopy and it was found that only 1.6 % of initial Mn dissolved in the filtrate solution. These results show that leaching of the Mn(Salen) complex from the catalyst sample during the liquid phase reaction was low and the catalyst was stable.

Recycling potential was studied according to the following method: the catalyst was separated from the reaction mixture after each experiment by filtration, washed with solvent and dried carefully before using it in the subsequent run. The catalyst was used for four cycles and there was a progressive loss of activity with a lowering in the conversion of benzyl alcohol that indicated that leaching of Mn(Salen) complex from the support had taken place. Therefore, the amount of Mn(Salen) complex loading was decreased in the sample and the activity of the catalyst in the next cycle decreased. The results are shown in Fig. 11. Conversion with only 10 % reduction was observed after four cycles. Therefore, these results show that the potential reusability of the catalyst is appropriate.

Conclusions

The SBA-15-pr-NH_2 Mn(Salen)Cl sample is an active agent in catalyzing the oxidation of benzyl alcohol with good conversion percentage and high selectivity by using TBHP as an oxidant. Only 0.1 g of the catalyst in mild conditions may be able to successfully carry out the oxidation reaction. This catalytic system in the polar

protic solvents such as acetonitrile gives the best conversion results and the potential reusability of the catalyst is excellent. The activity of the catalyst is a second order function with respect to the loading of manganese in the catalyst samples. In addition, alkyl peroxides proved to be very efficient and environmentally friendly oxidants since the by-products were just alkyl alcohols. It seems that this kind of catalysis system is very active, selective and suitable for the oxidation of benzyl alcohol.

References

1. R.A. Sheldon, J.K. Kochi, *Metal-Catalyzed Oxidation of Organic Compounds* (Academic, New York, 1981)
2. M. Hudlicky, *Oxidations in Organic Chemistry*, ACS Monograph Series (American Chemical Society, Washington, 1990)
3. M.P. Chaudhari, S.B. Sawant, Chem. Eng. J. **106**, 111 (2005)
4. C.L. Hill, A.L. Baumstark, *Advances in Oxygenated Processes*, vol. 1 (JAI, London, 1998)
5. S. Tsuruya, H. Miyamoto, T. Sakae, M. Masai, J. Catal. **64**, 260 (1980)
6. P. Sarmah, B.K. Das, P. Phukan, Catal. Commun. **11**, 932 (2010)
7. Q. Tang, X. Gong, P. Zhao, Y. Chen, Y. Yang, Appl. Catal. A **389**, 101 (2010)
8. Q. Tang, C. Wu, R. Qiao, Y. Chen, Y. Yang, Appl. Catal. A **403**, 136 (2011)
9. S. Tsuruya, Y. Okamoto, T. Kuwada, J. Catal. **56**, 52 (1979)
10. M. Arai, S. Nishiyama, S. Tsuruya, M. Masai, J. Chem. Soc. Faraday Trans. **92**, 2631 (1996)
11. H. Hayashibara, S. Nishiyama, S. Tsuruya, M. Masai, J. Catal. **153**, 254 (1995)
12. S. Sueto, S. Nishiyama, S. Tsuruya, M. Masai, J. Chem. Soc. Faraday Trans. **93**, 659 (1997)
13. R. Sumathi, K. Johnson, B. Viswanathan, T.K. Varadarajan, Appl. Catal. A **172**, 15 (1998)
14. N. Idaka, S. Nishiyama, S. Tsuruya, Phys. Chem. Chem. Phys. **3**, 1919 (2001)
15. V.R. Choudhary, P.A. Chaudhari, V.S. Narkhede, Catal. Commun. **4**, 171 (2003)
16. T.L. Stuchinskaya, I.V. Kozhevnikov, Catal. Commun. **4**, 417 (2003)
17. N. Lingaiah, K. Mohan Reddy, N.S. Babu, R.K. Narasimha, I. Suryanarayana, P.S. Sai Prasad, Catal. Commun. **7**, 245 (2006)
18. G.C. Behera, K.M. Parida, Appl. Catal. A Gen. **413**, 245 (2012)
19. R. Pillai, E. Sahle-Demessie, Appl. Catal. A **276**, 139 (2004)
20. V. Mahdavi, H.R. Hasheminasab, S. Abdollahi, J. Chin. Chem. Soc. **57**, 189 (2010)
21. E.F. Murphy, L. Schmid, T. Burgi, M. Maciejewski, A. Baiker, D. Gunther, M. Schneider, Chem. Mater. **13**, 1296 (2001)
22. I.C. Chisem, J. Rafelt, M.T. Shieh, J. Chisem, J.H. Clark, R. Jachuck, D. Macquarrie, C. Ramshaw, K. Scott, Chem. Commun. **18**, 1949 (1998)
23. B.M. Choudary, M.L. Kantam, B. Bharathi, P. Sreekanth, F. Figueras, J. Mol. Catal. A Chem. **159**, 417 (2000)
24. X.G. Wang, K.S.K. Lin, J.C.C. Chan, S. Cheng, J. Phys. Chem. B **109**, 1763 (2005)
25. M. Mureseanu, A. Reiss, I. Stefanescu, E. David, V. Parvulescu, G. Renard, V. Hulea, Chemosphere **73**, 1499 (2008)
26. S.A. Kozlova, S.D. Kirik, Microporous Mesoporous Mater. **133**, 124 (2010)
27. V. Mahdavi, M. Mardani, J. Chem. Sci. **124**, 1107 (2012)
28. V. Mahdavi, M. Mardani, M. Malekhosseini, Catal. Commun. **9**, 2201 (2008)
29. Y. Wang, F. Zhang, Y. Wang, J. Ren, C. Li, X. Liu, Y. Guo, Y. Guo, G. Lu, Mater. Chem. Phys. **115**, 649 (2009)
30. A. Stein, B.J. Melde, R.C. Schroden, Adv. Mater. **12**, 1403 (2000)
31. C.M. Crudden, M. Sateesh, R. Lewis, J. Am. Chem. Soc. **127**, 10045 (2005)
32. K. Srinivasan, P. Michaud, J.K. Kochi, J. Am. Chem. Soc. **108**, 2309 (1986)
33. B. Bosnich, J. Am. Chem. Soc. **90**, 627 (1968)
34. S.M. Crawford, Spectrochim. Acta. **19**, 255 (1963)
35. A. Domenech, P. Formentin, H. Garcia, M.J. Sabater, J. Phys. Chem. **106**, 574 (2002)

36. V. Mahdavi, S. Soleimani, Mater. Res. Bull. **51**, 153 (2014)
37. X. Wang, G. Wu, J. Li, N. Zhao, W. Wei, Y. Sun, J. Mol. Catal. A Chem. **276**, 86 (2007)
38. H.K. Kwong, P.K. Lo, K.C. Lau, T.C. Lau, Chem. Commun. **47**, 4273 (2011)
39. Q. Tang, X. Gong, C. Wub, Y. Chen, A. Borgna, Y. Yang, Catal. Commun. **10**, 1122 (2009)
40. H.Y. Sun, Q. Hua, F.F. Guo, Z.Y. Wang, W.X. Huang, Adv. Synth. Catal. **354**, 569 (2012)
41. V.R. Choudhary, D.K. Dumbre, B.S. Uphade, V.S. Narkhede, J. Mol. Catal. A Chem. **215**, 129 (2004)